Microstructural Studies on the Reoxidation Behavior of Nb-doped $SrTiO_3$ Ceramics

B. Rahmati[1], J. Fleig[2*], J. Maier[2], M. Rühle[1]

[1]Max Planck Institute for Metal Research, Stuttgart, Germany

[2]Max Planck Institute for Solid State Research, Stuttgart, Germany

Abstract

We report several structural and chemical phenomena that were observed after high temperature annealing (1200°C) of 5 at.% Nb-doped polycrystalline $SrTiO_3$ in oxygen. The oxidation led to the formation of islands on the surface which, depending on the surface orientation of the grains, exhibit characteristic shapes, densities, and lateral directions. A correlation between grain orientation and tendency towards island formation was found. Structure and composition of the islands and the bulk were investigated by transmission electron microscopy. The bulk interior of the oxidized $SrTiO_3$ was found to exhibit compositional changes and Sr-rich secondary phases were found at the triple grain junctions. The results are discussed in terms of the defect chemistry of $SrTiO_3$.

Keywords: Perovskites, $BaTiO_3$ and titanates, Surfaces, Defects, Electron microscopy

*corresponding author: j.fleig@fkf.mpg.de

I. Introduction

The electrical conductivity of donor-doped $SrTiO_3$ at room temperature strongly depends on the annealing conditions [1-5]. Annealing in reducing atmosphere leads to ceramics with electrons serving as counter charges to positively charged donors and thus yields high electron conductivity. After annealing at high oxygen partial pressure ($p(O_2)$) frozen-in Sr-vacancies (V''_{Sr}) prevail in the charge balance rendering the material insulating. This dependence of the materials properties on annealing conditions is, for example, exploited for the preparation of grain boundary layer capacitors [6].

The location of the Sr^{2+} ions, released during the Sr-vacancy formation at high $p(O_2)$, however, is still under debate. Several authors [1-5] assume the formation of Sr-rich phases (Ruddlesden-Popper phases, $Sr_{n+1}Ti_nO_{3n+1}$, [7]) in the ceramic samples to explain the generation of Sr-vacancies (i.e. sink of Sr-ions). Experimental evidence for the formation of Ruddlesden-Popper phases at the grain boundaries during reoxidation would therefore be highly desirable. Concerning the surface of $SrTiO_3$, a variation of $p(O_2)$ is known to lead to secondary phase formation [4,8-10]. Exposure of the (100) surface of single crystalline $SrTiO_3$ to oxygen at high temperatures (1200-1400°C), for example, has been observed to result in the formation of Sr-rich secondary phases on the surface [4,8].

The reoxidation (i.e. the change of the donor charge compensation) and, as a consequence, the V''_{Sr} formation in the bulk and the appearence of Sr-rich phases at the surface are closely related. Nevertheless, experimental studies dealing with both the oxidation behavior of surface and bulk are not available. Moreover, the role of the surface orientations on the oxidation behavior of $SrTiO_3$ has not been investigated in

detail. This paper deals with these shortcomings in the understanding of the reoxidation of donor-doped $SrTiO_3$.

II. Experimental

Nb-doped (5 mol%) polycrystalline $SrTiO_3$ with a stoichiometric composition of $SrTi_{0.95}Nb_{0.05}O_3$ was prepared from highly pure $SrCO_3$, TiO_2 and Nb_2O_5 powders (99.999%, Aldrich) by the mixed oxide route. The mixed powder was calcined at 1100 °C under air for 1 hour and isostatically pressed into a pellet under 680 MPa. The pellets were sintered under reducing atmosphere (5% H_2 + 95% Ar) at 1360 °C for 15 hours. The surface of the sintered samples was polished and exposed to an additional annealing step at a temperature of 1200°C under oxygen atmosphere either for 30 or 120 hours (reoxidation). In contrast to the slow heating/cooling rate during sintering (50°C/hour), rather higher heating/cooling rates were chosen during reoxidation (600 °C/hour).

Morphological and structural changes on the surface and in the bulk upon reoxidation were investigated by optical microscopy (LEICA, DMRM), scanning electron microscopy (SEM: LEO 438VP) and transmission electron microscopy (TEM: JEOL 2000FX). The compositional changes were determined by means of X-ray energy dispersive spectroscopy (EDS) integrated in the TEM. Orientation imaging microscopy (OIM) was used to obtain the different crystallite orientations of the polycrystalline sample; different grain orientations were chosen and deviations up to 5° were permitted.

III. Results and Discussion

1. Island Formation on the Surface

After oxidation for 30 hours, the surface of the initially reduced polycrystalline $SrTiO_3$ sample is partly covered by crystalline secondary phases referred to as "islands" (Fig. 1a). Depending on the orientations of the corresponding grains, the islands show characteristic shapes, specific lateral directions and strongly different densities. In the following, we discuss the dependency of the island density on the grain orientation. The island density for a given grain is expressed as the area of all islands normalized with respect to total surface area of the grain (ρ) and evaluated with the aid of a metallography software program (LEICA QWIN). The orientations of the grains were determined by OIM. The island densities are indicated in a standard orientation triangle (Fig. 1b). A clear correlation was found between surface orientations and island densities and the investigated surfaces can be classified into three groups:

i) (111) surface and similarly oriented surfaces such as (122) and (112) showed a high island density ($\rho > 20\%$).

ii) (001) surfaces and similarly orientated surfaces such as (013) and (114) exhibited low island density ($\rho < 6\%$).

iii) (011), (133) and (123) surfaces showed a moderate island density ($\rho \approx 15\%$).

Hence three orientation regimes can be defined which exhibit similar island formation densities (Fig. 1b). Each regime includes a low index surface, i.e. (001), (011) or (111) (located at the corner of the orientation triangle) and higher indexed surfaces with an inclinations of less than 20° compared to the low indexed surface. (Only the (012) surface does not fit to this classification rule).

The island densities (Fig. 1b) and thus the oxidation tendency of the surfaces correlate

with the surface energies reported in Ref. [10-12]. The highly polar (111) surface with high island density, for example, is characterized by a high surface energy which may be lowered by the formation of a secondary phase (island). Also orientation-dependent nucleation tendencies may influence the oxidation behavior.

With respect to structure and chemical composition of the islands spatially resolved electron diffraction and EDS measurements have been performed at two islands of different thickness (about 200 nm and 900 nm). The thinner island exhibited a smooth transition of the Ti/Sr ratio in the island from almost one (corresponding to $SrTiO_3$) to almost zero while preserving the perovskite structure of the $SrTiO_3$ bulk. The thicker island only contained Sr-cations and had a crystal structure strongly differing from $SrTiO_3$. A more detailed discussion of these results will be given in a forthcoming paper.

2) Grain interior

After reoxidation for 30 hours, an optically transparent area with an extension of about 50 to 70 μm was found beneath the surface of the polycrystalline sample. The optical transparency of this area indicates a strong decrease of the electron concentration, i.e. a change of the dopant compensation mechanism from electronic to ionic compensation. This region is therefore referred to as ‘‘reoxidized region’’. At larger distances from the surface (≈ 100 μm), the material is still reduced and thus optically non-transparent.

Successive chemical analysis was performed by EDS(TEM) from the surface through the reoxidized layer, down to the reduced region (Fig. 2). In the reoxidized region the Sr and Ti content differed considerably from that measured in the reduced region. While close to the surface an enrichment of Sr^{2+} and a deficiency of Ti^{4+} cations are

found, the concentration difference becomes smaller when approaching the reduced region. In a depth of ca. 50 µm even the reverse case, i.e. a reduced Sr^{2+} concentration and an enhanced Ti^{4+} level was found.

At a first glance this is surprising since one might expect a Sr-depletion close to the surface corresponding to the expected change from electronic to ionic charge compensation of the dopant. However, the strong oxygen chemical potential gradient between the surface and the bulk interior also acts as a driving force for a kinetic demixing in the $SrTiO_3$ bulk [13]. The prerequisite for such a demixing are sufficiently different cation mobilities which is fulfilled in the case of $SrTiO_3$, since Sr^{2+} cations are significantly more mobile than Ti^{4+} cations [3,14]. An enrichment of Sr^{2+} cations in the region with higher oxygen chemical potential, namely in the near-surface region is therefore in accordance with the model of kinetic demixing. This is the first experimental evidence of a kinetic demixing within the perovskite phase of $SrTiO_3$. A heterogeneous variant of kinetic demixing in $SrTiO_3$ is reported in Ref. [8] where it is suggested that high temperature annealing (1200°C-1400°C) results in Sr-rich islands at the surface and Ti-rich near-surface region (on a nm-scale). Here, however, we consider a non-heterogeneous effect (without phase separation) taking place on the length scale of several 10 µm.

With respect to the structural realization of the varying Sr/Ti ratio (within a single phase) a final conclusion cannot be drawn. We suggest either anti-site defects or intergrowth layers. In the case of anti-site defects excess Sr^{2+} cations would replace Ti^{4+} and result in $Sr_{Ti}^{''}$ defects which may (instead of $V_{Sr}^{''}$) ionically compensate the charge of $Nb_{Ti}^{\bullet}$. Far away from the surface, excess Ti^{4+} cations may occupy Sr^{2+} lattice sites and result in $Ti_{Sr}^{\bullet\bullet}$ defects. It is unclear in how far the large difference in the ionic radii of Sr^{2+} and Ti^{4+} impedes the formation of significant concentrations of

anti-site defects at 1200 °C and Ti- or Sr-rich intergrowth layers (without phase separation) may therefore also be considered as an explanation for the profiles measured.

3) Grain boundaries

In the reoxidized sample (120 hours annealing) secondary phases could be identified at the triple grain junctions (Fig. 3). Compared to the neighboring bulk (Fig. 3a), the diffraction pattern of the secondary phase in [100]-zone axis (Fig. 3b) shows an additional spot along the [001] direction. Super-reflections were also found in the [210]-zone axis. The electron diffraction pattern of the secondary phase fits to that of Sr_2TiO_4 [15]. Assuming the secondary phase to be Sr_2TiO_4, the lattice constants a = b = (3.983 ± 0.014) Å and c = (11.65 ± 0.23)Å can be derived and fit well to literature values (a = b = 3.983 Å; c = 11.80 Å, [8]).

Sr_2TiO_4 belongs to the homologous series $Sr_{n+1}Ti_nO_{3n+1}$ (n = 1, 2, 3, ...), which is well-known as Ruddlesden-Popper phases [7] often resulting if $SrTiO_3$ powders are prepared with large excess of $SrCO_3$. The Sr_2TiO_4 intergranular phase (n = 1) in the stoichiometric $SrTi_{0.95}Nb_{0.05}O_3$ samples observed after reoxidation, is related to the Sr-ions expelled according to the change of the charge compensation mechanism for donors from electronic to ionic. Owing to the lack of data, the existence of the other members of the $Sr_{n+1}Ti_nO_{3n+1}$ series can neither be proven nor excluded. Such a Sr-rich secondary phase at grain boundaries upon reoxidation has often been predicted in literature [1-5] but to the best of our knowledge this is the first explicit evidence for its formation. More details on these investigations are given in a forthcoming paper.

IV. Conclusions

Reoxidation phenomena taking place at surfaces, in the grain interior and at grain boundaries of reduced Nb-doped polycrystalline $SrTiO_3$ have been discussed:

The properties (density, shape, size, composition, etc.) of Sr-rich islands formed on the surface of reoxidized polycrystalline $SrTiO_3$ depend significantly on the surface orientation of the grains. With respect to the island frequency (low, moderate and high), three groups of surface orientations were defined and related to (001), (011) and (111) orientations. The different island formation tendencies correspond to different surface energies.

A pronounced cationic demixing in $SrTiO_3$ is found on a length scale of several 10 μm. Whereas more mobile Sr^{2+} ions enrich in the near-surface region, less mobile Ti^{4+} ions accumulate in the bulk region far from the surface. The strong oxygen chemical potential difference between the surface and the bulk interior is assumed to be the driving force of the kinetic demixing and the peculiar non-stoichiometries.

A Sr-rich secondary phase (Sr_2TiO_4, a member of Ruddlesden-Popper phases) was identified at the triple junctions between grains. The formation of Sr_2TiO_4 acts as sink for Sr^{2+} ions expelled from the $SrTiO_3$ grains upon reoxidation.

References

1. Daniels, J. & Härdtl, K.H., Electrical conductivity at high temperatures of donor-doped $BaTiO_3$ ceramic. *Phillips Res. Repts*., 1976, **31,** 489-504.
2. Eror, N.G. & Balachandran, U., Self-compensation in lanthanum-doped $SrTiO_3$. *J. Solid State Chem.*, 1981, **40**, 85-91.
3. Moos, R. & Härdtl, K. H., Defect chemistry of donor-doped and undoped $SrTiO_3$ ceramic between 1000 and 1400°C. *J. Am. Ceram. Soc.,* 1997, **80**, 2549-2562.
4. Meyer, R. & Waser, R., Cationic surface segregation in donor-doped $SrTiO_3$ under oxidizing conditions. *J. Electroceramics*, 2002, **9**, 101-110.
5. Menesklou, W., Schreiner, H. J., Härdtl, K. H., High temperature oxygen sensors based on doped $SrTiO_3$. *Sensors and Actuators* B, 1999, **59**, 184-189.
6. Fujimoto, M. & Kingery, W. D., Microstructure of $SrTiO_3$ internal boundary layer capacitors. *J. Am. Ceram. Soc*., 1985, **68**, 169-173.
7. Ruddlesdon, S.N. & Popper, P., New compounds of the K_2NiF_4. *ActaCrystallogr.*, 1957, **10,** 538-547.
8. Szot, K. & Speier, W., Surface of reduced and oxidized $SrTiO_3$ from atomic force microscopy. *Phys. Rev. B*, 1999, **60**, 5909-5926.
9. Wei, H. & Beuermann, L., Study of SrO segregation on $SrTiO_3$ (100) surfaces. *J.Eur. Ceram. Soc.*, 2001, **21**, 1677-1680.
10. Liang, Y. & Bonnell, D. A., Structures and chemistry of the annealed $SrTiO_3$ (100) surface. *Surf. Sci.*, 1994, **310**, 128-134.
11. Noguera, C., *Physics and Chemistry at Oxide Surfaces*, Cambridge University Press, 1996, pp. 42-49.
12. Sano, T. & Saylor, D. M., Surface energy anisotropy of $SrTiO_3$ at 1400°C in air. *J. Am. Ceram. Soc.*, 2003, **86**, 1933-1939.
13. Schmalzried, H. & Laqua, W., Crystalline oxide solid solutions in oxygen potential gradients. Z. *Naturforsch.*, 1979, **34A**, 192-199.
14. Chan, N. H., Sharma, R. K. & Smyth, D. M., Nonstoichiometry in $SrTiO_3$. *J. Electroceram. Soc.:* Solid-State Science and Technology, 1981, **128**, 1762-1768.
15. Tilley, R .J . D., An electron microscopy study of perovskite-related oxides in the Sr-Ti- O system. *J. Solid State Chem.,* 1977, **21**, 293-301.

Figure Captions

Fig. 1.: (a) Optical micrographs of the reoxidized surface of polycrystalline $SrTi_{0.95}Nb_{0.05}O_3$ with islands on the surface.

(b) The dependence of the island density (ρ in %) on the surface-orientation <*hkl*> is presented by standard orientation triangle. The surfaces are classified in three orientation regimes with similar island density (striped regions). Orientation deviations up to 5° were permitted in the OIM analysis.

Fig. 2: Cation composition beneath the surface in the reoxidized and the reduced region measured by EDS (TEM). While the Nb^{5+} concentration is almost constant, Sr^{2+} and Ti^{4+} cations undergo demixing in the reoxidized region. The dashed lines relate to the concentrations of cations in the reduced sample (The data are normalized to the reduced sample asumming [Sr] = 50 at%; [Ti] = 47.5 at%; [Nb] = 2.5 at%).

Fig. 3: Bright-field TEM micrograph of the bulk of the reoxidized $SrTi_{0.95}Nb_{0.05}O_3$ sample viewed along the [100]-zone axis. A secondary phase is present at the triple junction. Insets show electron diffraction patterns of **a)** the matrix in [100]-zone axis, and of the secondary phase in **b)** [100]-zone axis.

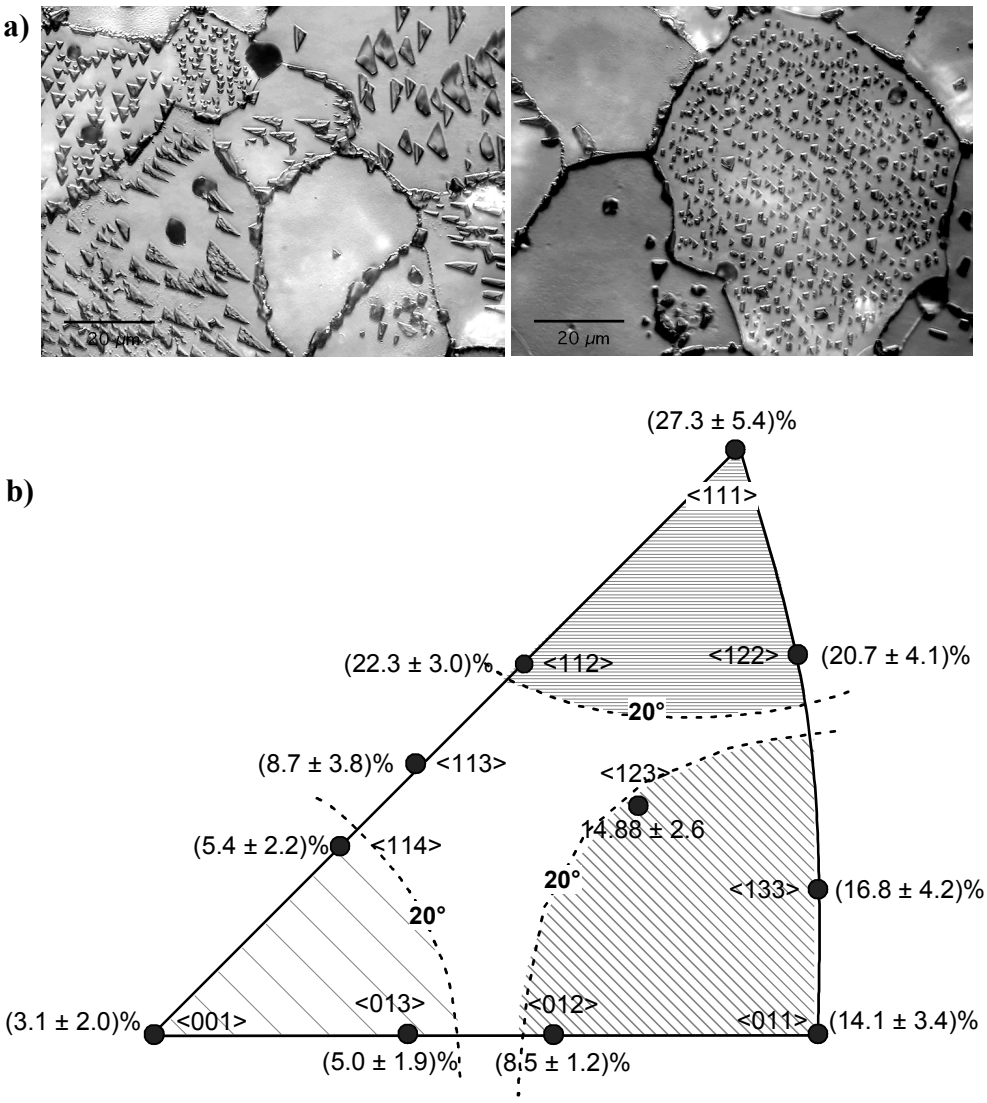
a)
20 μm
20 μm
b)
(27.3 ± 5.4)%
<111>
(22.3 ± 3.0)%
<112>
<122>
(20.7 ± 4.1)%
20°
(8.7 ± 3.8)%
<113>
<123>
(4.88 ± 2.6
(5.4 ± 2.2)%
<114>
20°
20°
<133>
(16.8 ± 4.2)%
(3.1 ± 2.0)%
<001>
<013>
<012>
<011>
(14.1 ± 3.4)%
(5.0 ± 1.9)%
(8.5 ± 1.2)%

Figure 1

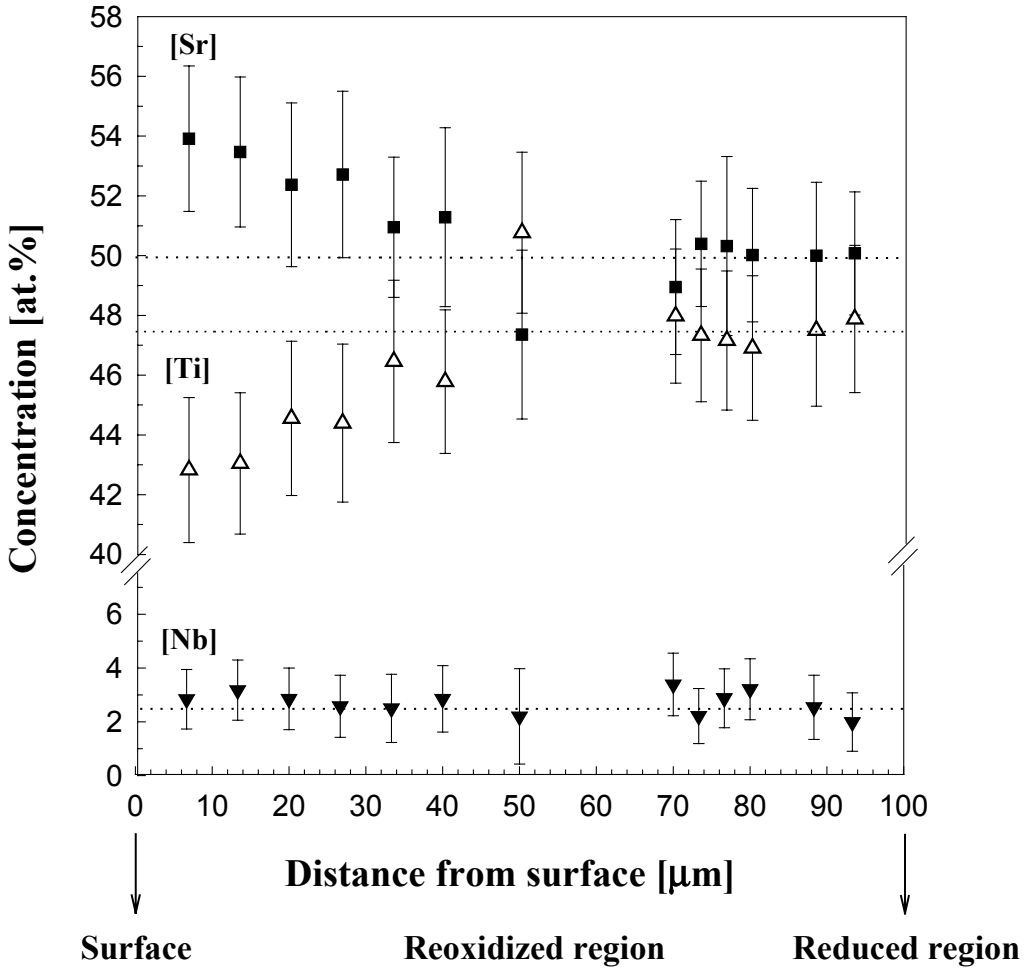
[Sr]
[Ti]
[Nb]
Concentration [at.%]
Distance from surface [μm]
Surface
Reoxidized region
Reduced region

Figure 2

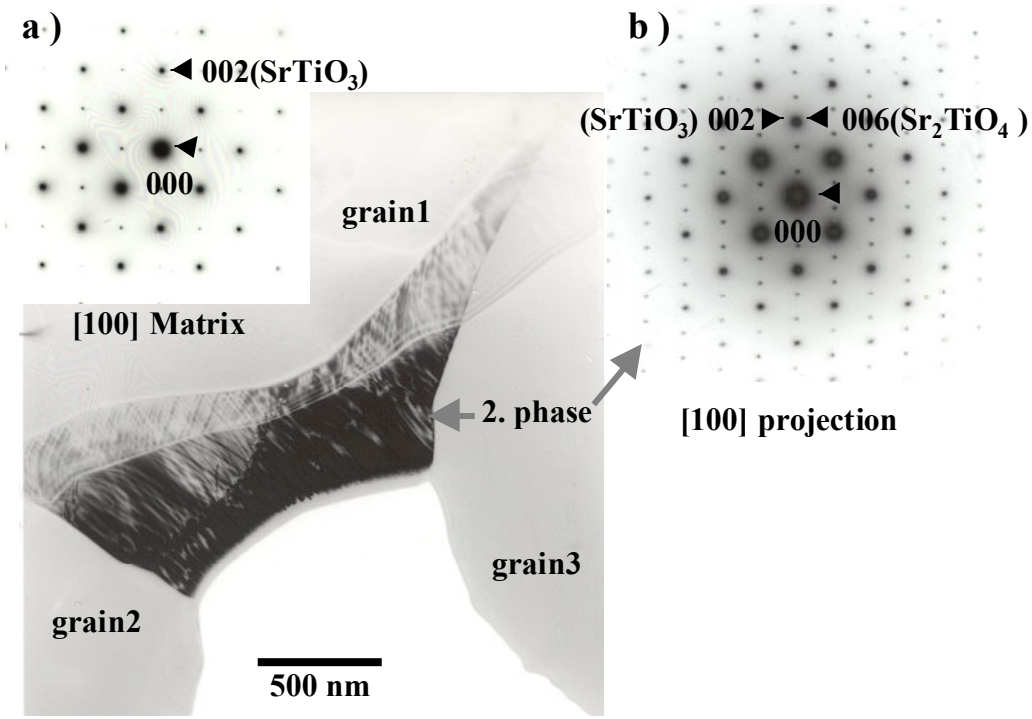
a)
002(SrTiO3)
000
[100] Matrix
grain1
2. phase
grain3
grain2
500 nm
b)
(SrTiO3) 002
006(Sr2TiO4)
000
[100] projection

Figure 3